Hydro-structural stability investigation of a 100 MW Francis turbine based on experimental tests and numerical simulations

IOP Conf. Series: Earth and Environmental Science **405** (2019) 012006 doi:10.1088/1755-1315/405/1/012006

Hydro-structural stability investigation of a 100 MW Francis turbine based on experimental tests and numerical simulations

J Decaix[1], V Hasmatuchi[2], M Titzschkau[3], L Rapillard[2], C Münch-Alligné[2]

[1] Institute of Sustainable Energy, School of Engineering, HES-SO Valais-Wallis, Rawil 47, Sion, Switzerland
[2] Institute of Systems Engineering, School of Engineering, HES-SO Valais-Wallis, Rawil 47, Sion, Switzerland
[3] Kraftwerke Oberhasli AG, Grimsel Hydro, CH-3862 Innertkirchen, Switzerland

E-mail: `jean.decaix@hevs.ch`

Abstract. This work focuses on a 100 MW Francis turbine prototype, part of one of the four horizontal ternary groups of Grimsel 2 PSPP, in Switzerland. Due to the massive integration of new renewable energy, the number of daily starts/stops of the machines has increased. Consequently, cracks on the runner blades of the Francis turbines have been noticed, without a clear explanation regarding the phenomenon responsible for their onset.
To identify the main stress-full operating condition causing these cracks, the full turbine hill chart has been covered during the *in situ* measurement campaign including start-up, speed no-load, deep part load, best efficiency, full load and shut-down operating conditions. Then hydro-structural stability diagnosis diagrams of the prototype have been established for the whole operating range of the turbine. In addition, CFD numerical simulations for different operating conditions, along with FEM structural and modal analysis of the runner, have been carried out.
The onboard measurements evidenced the highest mechanical stresses on the runner blades at speed no-load operating condition. This conclusion is supported by CFD and FEM analysis, which put in evidence the possible excitation of one of the runner's eigen frequency by the fluctuations of the pressure field.

1. Introduction

The development in the last decades of wind and solar energy, characterised by their stochastic behaviour, led to electricity network instabilities [1]. To mitigate the impact of these new renewable energy resources, hydraulic turbines and pump-turbines are becoming key technical components due to their ability to propose storage capacity [2] as well as flexibility [3]. However, flexibility is related to the extension of the hydraulic machines operating range, which is a challenging task, see for instance the study of Lowys *et al.* [4] and the conclusions of the Hyperbole FP7 European project [5]. Indeed, the increase in flexibility leads to the increase in the number of start-up, stand-by and shut down operations. Consequently, the hydraulic machines undergo strong dynamic loads resulting in a reduction of their lifespan [6, 7]. In order to cope with the challenge of flexibility, experimental investigations are required both at model [8, 9] and at prototype [10, 11] scale. In parallel, numerical tools such as Finite Elements Method (FEM), Computational Fluid Dynamics (CFD) and Fluid Structure Interaction (FSI) have become more and more reliable to investigate the behaviour of the hydraulic machines [12]. The present paper focuses on both experimental [13] and FEM [14, 15] investigations of the phenomenon responsible for the appearance of the cracks on the runner blade of a ternary unit at a prototype scale, such as investigated by Muller [16]. First, the case study is briefly described. Then, the experimental and numerical set up are provided. Finally, the results are presented and discussed.

2. Case study

The case study is the Grimsel 2 pumped-storage power plant operated by KWO [17] and built between 1974 and 1980 in Switzerland. This power plant is equipped with four 100 MW ternary groups: a horizontal-axis motor/generator, a Francis turbine and a centrifugal pump. The specific speed of the Francis turbine runner is $\nu = 0.247$. The speed and discharge factors of the turbine at the Best Efficiency Point (BEP) are respectively $n_{ED} = 0.271$ and $Q_{ED} = 0.183$. The main efforts are dedicated to the investigation of the turbine mode, since after a given number of operation cycles, some cracks have been observed on the runner (made in steel G-X5 Cr Ni 13 4) at the junction between the trailing edge of the blades and the hub. The phenomenon responsible for the development of the cracks is not yet clearly identified even if it seems related to the increase in the number of start-up, stand-by and shut-down procedures per year.

3. Experimental setup

The philosophy of the employed *in situ* instrumentation to identify the possible harmful structural conditions for the turbine runner consists of synchronised measurements between the rotating and the stationary frames of the machine [18]. To this end, an autonomous digitizer from Gantner has been installed in a sealed chamber placed into the runner cone (see figure 1). Strain gauges placed on four consecutive impeller blades along with accelerometers and tachometers have been connected to the acquisition system.
The stationary frame instrumentation consists mainly on two synchronised National Instruments digitizers connected to several monitoring sensors placed on both the turbine and the pump of the unit. The frequency of the acquisition for all connected sensors has been set to 10 kHz. Three pressure sensors, one inclinometer, one flowmeter, one tachometer, two proximity sensors, one microphone and several accelerometers have been used to capture the source of the instabilities in the same time with the rotating frame instrumentation. As shown in Botero et al. [19], the hydrodynamic instabilities should be normally detected from outside using only non-intrusive instrumentation, such as accelerometers or microphones.

4. FEM setup

FEM is used to perform a modal analysis and a structural analysis of the runner using the Ansys Workbench 17.2 environment. Regarding the modal analysis, the computational domain consists of the runner and a surrounding volume of water (see figure 2 left) and it is meshed with 350'000 tetrahedral elements (see figure 2 right). Regarding the structural analysis performed at BEP and speed no-load (SNL), only the runner is considered, for which the mesh is refined up to 4.5 million of nodes. For both analysis, a fixed support condition is set at the junction between the runner and the shaft (see figure 2 middle). For the structural analysis, the pressure field extracted from the CFD simulations is applied on the runner blades.

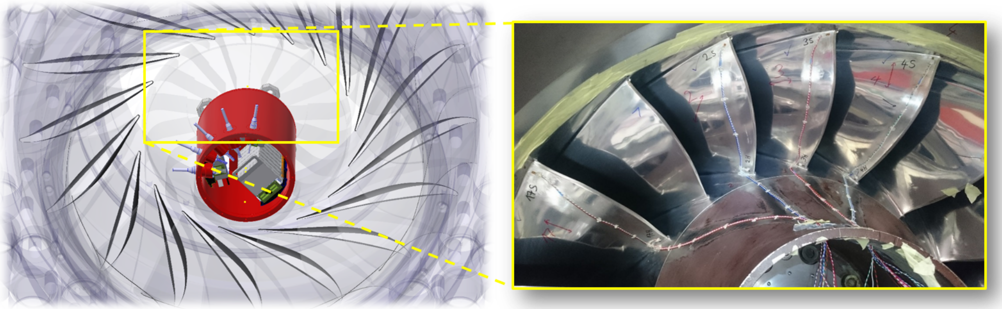

Figure 1. Onboard measurements system along with the strain gauges installed in the runner.

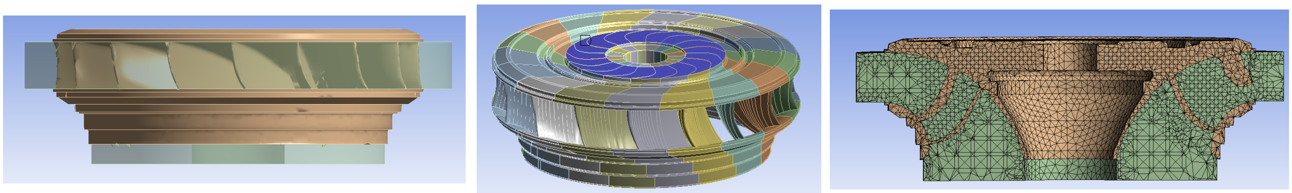

Figure 2. FEM computational domain (left), location of the fixed support boundary condition (centre) and mesh (right).

5. Results

5.1. Experimental results

The *in situ* measurements campaign focused mainly on the full operating range of the turbine for a given testing head condition (including the start-up in pump mode). In figure 3, the signals of two strain gauges installed on one of the turbine runner blade (namely BL17) close to the hub and to the shroud (measurement direction parallel to the blade trailing edge) along with the signal of one accelerometer during the start-up procedure are provided for one complete turbine start-to-stop cycle.

Chronologically, the turbine filling and start-up, followed by the synchronization of the generator with the electrical network, then stable part load operation followed by the shut down procedure and the draining can be easily identified. Both the fluctuations of the strain as well as the vibrations of the runner evidence larger amplitudes during the synchronisation of the generator with the network and during the shutdown phase. The maximum amplitude of strain occurs at SNL operating point during the synchronization of the generator with the network as well as during the shutdown (phenomenon already shown by [7, 20]). These harsh operating conditions, that accelerate the shortening of the runners remaining lifetime, are encountered each time the turbine is started and stopped for several tens of seconds (up to few minutes in the worst case). Regarding the frequency of these fluctuations, despite the fact that it is very close to the first harmonic of the blade passing frequency, the observed value seems to be the response of one of the runner eigenmodes. The amplitude of fluctuations for this strain direction is larger at the shroud than at the hub blade side. Moreover, a sub-synchronous frequency (compared to the runner rotational frequency) is observed in the variation of the strain fluctuation amplitude.

Then, in figure 4, considering the same SNL operating point, one may state that the same predominant oscillation ($f/f_n = 48.9$) is observed not only on the signal of the accelerometer installed in the runner, but also in the signal of the accelerometer installed on the turbine casing as well as in the ones coming from the microphone and from the proximity sensor. This result

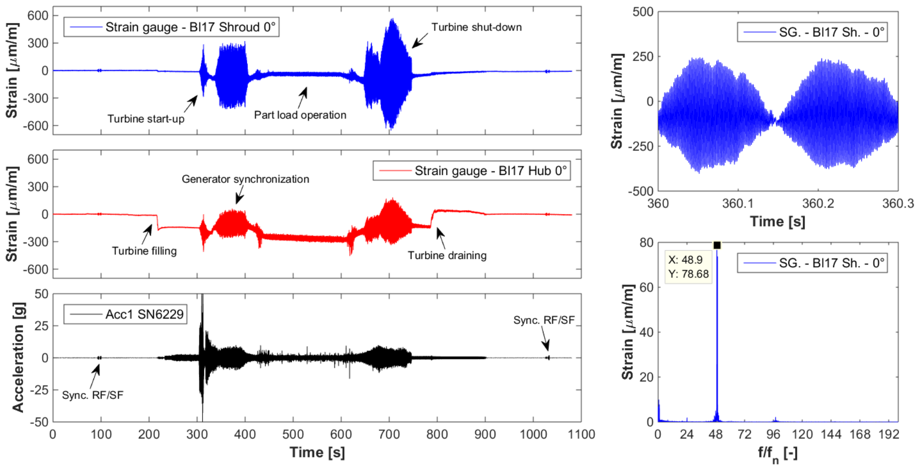

Figure 3. Evidence of harmful structural loading of the turbine runner blades during the normal start-up and shut down procedures - signals recorded with the on-board instrumentation ([18]).

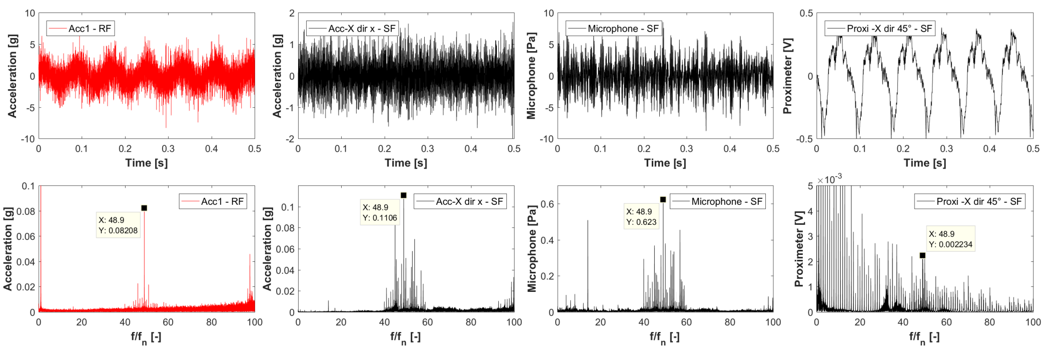

Figure 4. Identification of the main harmful structural loading fluctuation of the turbine runner blades during the SNL operation in the signals of the on-board accelerometer (left) and of the non-intrusive instruments: accelerometer, microphone and proximity sensor [14].

shows the capability of detecting such harmful conditions using only a simplified non-intrusive instrumentation set.

5.2. FEM results

The frequency and the modes of the runner have been investigated by a modal analysis (see table 1). It is noticeable that the bending mode characterised by a dimensionless frequency (*i.e* the frequency of the mode divided by the runner frequency) of 49 and 4 nodal diameters matches the frequency observed on the experimental signals.

The structural analysis provides the elastic strains on the runner blade due to the pressure load of the fluid. For each operating point, the maximum value of the elastic strain is located at the junction between the blade trailing edge and the hub as shown in figure 5. Among a large part of the runner, the elastic strain is between one and two order of magnitude higher at the SNL operating point than at the BEP. However, the maximum elastic strain is of 2'150 μm/m at the BEP and decreases to 1'000 μm/m at the SNL operating point. In the region corresponding to the position of the strain gauges, the values of the elastic strain are around 100 μm/m at

Table 1. Frequencies and types of the mode of the runner. Modal analysis results.

Dimensionless frequency	Type of mode	Number of nodal diameters
27.3	bending	1
29.0	bending	2
30.2	torsional	0
41.0	bending	3
44.2	torsional	0
49.0	bending	4
51.6	bending	5

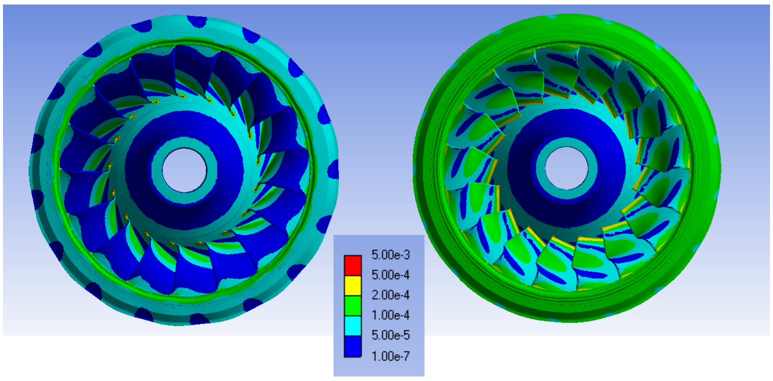

Figure 5. Contours of the equivalent elastic strain in m/m plotted on the deformed runner. BEP (left) and SNL (right) operating points. Structural results.

BEP and 250 μm/m at SNL.

6. Discussion

The carried out measurements and numerical simulations, allow us proposing a scenario to explain the apparition of the cracks at the junction between the trailing edge of the runner blade and the hub. Based on the measurements, fluctuations of the elastic strain, with a large peak to peak amplitude, are observed mainly during the turbine start-up and during the turbine shut-down when the guide vanes are again closed towards 2°. The frequency of these harsh fluctuations is close to 49 f_n, which is also the frequency of one of the bending mode computed by the modal analysis of the runner. For this operating point, it is possible that this eigen mode is partially excited. The measured amplitude of the elastic strain is around 250 μm/m, which corresponds to an amplitude of the stresses of $\sigma_a \approx 50$ MPa. The structural analysis provided an estimation of the mean stress at the position of the strain gauges around $\sigma_m = 50$ MPa. Using the Soderberg's criterion, the equivalent stress fluctuations σ_d is equal to 57 MPa (taking an elastic limit $R_{p0,2} = R_e = 639$ MPa [21]). Reporting this value of σ_d in the Wholer curve of the runner's steel [21], an estimation of the number of cycles after which cracks could appear is around 2.10^8. Based on both an averaged-time duration at which the turbine operates at SNL (let's say 60 seconds) and the frequency of the phenomenon observed, the lower limit of the number of cycles could be reached after approximately 5'500 starts. For the considered runner, this number of start and stop cycles has been overtaken.

7. Conclusion

An experimental investigation of a Francis turbine prototype, part of a ternary group, have been carried using both onboard runner and external instrumentation. The measurements put in evidence the existence of harmful conditions for the runner during the synchronization of the turbine with the grid at SNL. In addition, a FEM modal analysis allowed us computing the eigen mode of the turbine runner. The one way coupling between CFD and FEM allowed us estimating the runner deformation and the mean stresses due to the flow pressure. Using all the experimental and numerical information, a scenario for the onset of the harmful conditions has been provided. This scenario suggests that an eigen mode of the runner could be partially excited leading to the apparition of the cracks due to the overtaking of the fatigue limit of the runner. However, the source of the excitation is still missing in the proposed scenario and will be a task for a future work.

Acknowledgments

This project is part of the research program FLEXSTOR (Solutions for flexible operation of storage hydropower plants in changing environment and market conditions) of the Swiss Competence Centre for Energy Research - Supply of Electricity (SCCER-SoE, Phase II), co-funded by the Swiss Commission for Technology and Innovation (grant CTI - 17902.3 PFIW-IW) and by Kraftwerke Oberhasli AG.

References

[1] Vu T L and Turitsyn K 2016 *IEEE Int. Conf. on Sustainable Energy Technologies (ICSET)* pp 7–12
[2] Pérez-Díaz J I, Chazarra M, García-González J, Cavazzini G and Stoppato A 2015 *Renewable and Sustainable Energy Reviews* **44** 767–784 ISSN 13640321
[3] Huertas-Hernando D and *et al* 2017 *Wiley Interdisciplinary Reviews: Energy and Environment* **6** 1–20
[4] Lowys P Y, Guillaume R, André F, Duparchy F, Castro Ferreira J, Ferreira da Silva A and Duarte F 2014 *Hydro 2014* (Como, Italy)
[5] Hyperbole consortium 2017 Final Report Summary - HYPERBOLE `https://cordis.europa.eu/result/rcn/208601_en.html` , Last accessed on 2018-08-10
[6] Seidel U, Mende C, Hübner B, Weber W and Otto A 2014 *IOP Conf. Series: Earth and Environmental Science* **22** 032054
[7] Coutu A and Chamberland-Lauzon J 2015 *Int. J. on Hydropower & Dams* **2** 90–93
[8] Lowys P Y, Paquet F, Couston M, Farhat M, Natal S and Avellan F 2002 *Proc. of the 21st IAHR Symp.* pp 873–880
[9] Hasmatuchi V 2012 *Hydrodynamics of a Pump-Turbine Operating at Off-Design Conditions in Generating Mode* Ph.D. thesis EPFL No. 5373
[10] Gagnon M, Tahan S A, Bocher P and Thibault D 2012 *IOP Conf. Series: Earth and Environmental Science* **15** 022005
[11] Egusquiza E, Valentín D, Presas A and Valero C 2017 *J. of Physics: Conf. Series* **813** 012037
[12] Keck H and Sick M 2008 *Acta Mechanica* **229** 211–229
[13] Hasmatuchi V, Titzschkau M, Decaix J, Avellan F and Münch-Alligné C 2017 *SCCER-SoE Annual Conf.* (Birmensdorf, Switzerland)
[14] Decaix J, Hasmatuchi V, Titzschkau M, Rapillard L, Manso P, Avellan F and Münch-Alligné C 2019 *IOP Conference Series: Earth and Environmental Science* **240** 082014 ISSN 1755-1315
[15] Decaix, Jean and Hasmatuchi, Vlad and Titzschkau, Maximilian and Münch-Alligné, Cécile 2018 *Applied Sciences* **8** ISSN 2076-3417
[16] Müller C, Staubli T, Baumann R and Casartelli E 2014 *IOP Conf. Series: Earth and Environmental Science* **22** 032053
[17] Schlunegger H and Thöni A 2013 *Hydro 2013* (Innsbruck, Austria)
[18] Hasmatuchi V, Decaix J, Titzschkau M and Münch-Alligné C 2018 *Hydro 2018*
[19] Botero F, Hasmatuchi V, Roth S and Farhat M 2014 *Mechanical Systems and Signal Processing* **48** 162–173
[20] Gagnon M, Jobidon N, Lawrence M and Larouche D 2014 *IOP Conf. Series: Earth and Environmental Science* **22** 032022
[21] Sonsino C M and Dieterich K 1990 *Materials and Corrosion* **41** 330–342